Plant Cell Rep (2017) 36:1655–1666
DOI 10.1007/s00299-017-2181-5

ORIGINAL ARTICLE

# *Wax Crystal-Sparse Leaf 4*, encoding a β-ketoacyl-coenzyme A synthase 6, is involved in rice cuticular wax accumulation

**Lu Gan[1] · Shanshan Zhu[1] · Zhichao Zhao[1] · Linglong Liu[2] · Xiaole Wang[1] · Zhe Zhang[1] · Xin Zhang[1] · Jie Wang[1] · Jiulin Wang[1] · Xiuping Guo[1] · Jianmin Wan[1,2]**

Received: 21 May 2017 / Accepted: 9 July 2017 / Published online: 21 July 2017


**Abstract**

***Key message* *WSL4* encodes a KCS6 protein which is required for cuticular wax accumulation in rice.**

*Abstract* Very long chain fatty acids (VLCFAs) are essential precursors for cuticular wax biosynthesis. VLCFA biosynthesis occurs in the endoplasmic reticulum and requires the fatty acid elongase (FAE) complex. The β-ketoacyl-coenzyme A synthase (KCS) catalyzes the first step of FAE-mediated VLCFA elongation. Here we characterized the *Wax Crystal-Sparse Leaf 4* (*WSL4*) gene involved in leaf cuticular wax accumulation in rice. The *wsl4* mutant displayed a pleiotropic phenotype including dwarfism, less tiller numbers and reduced surface wax load. Map-based cloning and nucleotide sequencing results revealed that *wsl4* carried a single nucleotide substitution in the second exon of a putative *KCS6* gene, encoding one subunit of the FAE complex for VLCFAs. Genetic complementation confirmed that the mutation in *WSL4* was responsible for the phenotype of *wsl4*. *WSL4* was constitutively expressed in various rice tissues and localized in the endoplasmic reticulum. Both *WSL4-RNAi* transgenic lines and *WSL4* knocked-out mutants exhibited wax-deficient phenotypes similar to the *wsl4* mutant. These data indicate that *WSL4* is required for cuticular wax accumulation in rice.

**Keywords** Rice (*Oryza sativa*) · Cuticular wax · *Wax Crystal-Sparse Leaf 4* · β-Ketoacyl-coenzyme A synthase 6 · Fatty acid elongase

**Abbreviations**

| | |
|---|---|
| CER | Eceriferum |
| CoA | Coenzyme A |
| ECR | Enoyl-CoA reductase |
| ER | Endoplasmic reticulum |
| FAE | Fatty acid elongation |
| GC–MS | Gas chromatography–mass spectrometry |
| GFP | Green fluorescent protein |
| GUS | β-Glucuronidase |
| HCD | β-Hydroxyacyl-Coa dehydratase |
| KCR | β-Ketoacyl-CoA reductase |
| KCS | β-Ketoacyl-CoA synthase |
| RNAi | RNA interference |
| SEM | Scanning electron microscope |
| TEM | Transmission electron microscopy |
| ORF | Open reading frame |
| qRT-PCR | Quantitative RT-PCR |
| UBQ | Ubiquitin |
| VLCFAs | Very long chain fatty acids |
| WSL | Wax Crystal-Sparse Leaf |

Communicated by Qiao Zhao.

Lu Gan, Shanshan Zhu, and Zhichao Zhao contributed equally to this work.

**Electronic supplementary material** The online version of this article (doi:10.1007/s00299-017-2181-5) contains supplementary material, which is available to authorized users.

✉ Jianmin Wan
wanjianmin@caas.cn; wanjm@njau.edu.cn

[1] National Key Facility for Crop Gene Resources and Genetic Improvement, Institute of Crop Science, Chinese Academy of Agricultural Sciences, Beijing 100081, China

[2] National Key Laboratory for Crop Genetics and Germplasm Enhancement, Jiangsu Plant Gene Engineering Research Center, Nanjing Agricultural University, Nanjing 210095, China

## Introduction

The aerial surfaces of land plants are covered with a cuticle, a continuous hydrophobic layer mainly consisting of two major types of lipids, cutin and waxes (Kunst and Samuels 2009; Buschhaus and Jetter 2012). The cutin is a polymer which consists of omega and mid-chain hydroxy and epoxy C16 and C18 fatty acids, as well as their derivatives (Samuels et al. 2008). Wax compounds are deposited both within (intracuticular waxes) and on the surface (epicuticular waxes) of the cutin matrix, where they can form as crystals (Jetter and Schaffer 2001; Kannangara et al. 2007). The waxes protect plants from non-stomatal water loss, pathogen invasion and other stresses such as dust, insects and frost (Sieber et al. 2000; Aharoni et al. 2004; Sturaro et al. 2005; Li-Beisson et al. 2013; Espana et al. 2014).

Cuticular waxes are mainly composed of VLCFAs and their derivatives including aldehydes, primary and secondary alcohols, alkanes, ketones and wax esters (Yeats and Rose 2013). The biosynthesis of wax occurs exclusively within the plastid of epidermal cells where the C16 and C18 fatty acids were produced. Then the two fatty acids are used as precursors for the generation of VLCFAs up to 38 carbons followed by the decarbonylation and acyl reduction pathways to derive all the components (Shepherd and Wynne Griffiths 2006). The extension of C16 and C18 fatty acids to VLCFAs occurs on the endoplasmic reticulum (ER) via the fatty acid elongation (FAE) complex (Lee and Suh 2013). The FAE includes four enzymes: a β-ketoacyl-CoA synthase (KCS), a β-ketoacyl-CoA reductase (KCR), a β-hydroxyacyl-CoA dehydratase (HCD) and an enoyl reductase (ECR). Each elongation cycle involves four successive enzymatic reactions: condensation, reduction, dehydration and reduction, which together extend the substrate's carbon chain by a C2 unit in one cycle (Haslam and Kunst 2013).

Unlike the other three enzymes, the KCS condensing enzyme showed strict substrate specificity and was considered as the cycle's rate-limiting enzyme (Paul et al. 2006). The *Arabidopsis* genome contains 21 FAE-like KCS members, which have been found to have different substrate specificites, such as FAE1 (James et al. 1995), KCS1 (Todd et al. 1999), CER6/CUT1/KCS6 (Millar et al. 1999; Fiebig et al. 2000; Hooker et al. 2002), KCS2/DAISY (Lee et al. 2009), KCS20 (Lee et al. 2009) and KCS9 (Kim et al. 2013). However, to date, only a few KCS genes have been cloned in rice, like *WSL1* (Yu et al. 2008), *ONI1* (Ito et al. 2011) and *ONI2* (Tsuda et al. 2013).

Here, we used map-based cloning to identify the rice *Wax crystal-sparse leaf 4* (*WSL4*) gene that involved in leaf cuticular wax accumulation. The *wsl4* mutant exhibited reduced epicuticular wax crystals on the leaf surface compared to its wild type (WT). Amino acid sequence analysis suggested that WSL4 was a member of the KCS family. *WSL4* was constitutively expressed in rice and localized in the ER, where the FAE complex was localized. Further study showed both knocks-down and knocks-out of *WSL4* reduced cuticular wax loads on leaves. Together, all these data indicate that WSL4 is involved in wax biosynthesis in rice.

## Materials and methods

### Plant material and growth conditions

*wsl4*, a rice leaf wax deficient mutant, is a tissue culture-induced mutation of Japonica cv Nipponbare. For fine mapping of the *wsl4* gene, the *wsl4* mutant was crossed with *indica* cv Yuewanxian to construct an $F_2$ mapping population. All rice plants used in this study were cultivated in the experimental field under normal growth conditions at Changping (Beijing, China) or Sanya (Hainan, China).

### Scanning and transmission electron microscopy

For scanning electron microscopy (SEM) analysis, leaves and leaf sheaths were air dried. Epicuticular wax crystals were imaged on a HITACHI 8100 variable-pressure scanning electron microscope. To observe the transverse cuticle structure of *wsl4*, transmission electron microscopy (TEM) analysis was carried out as described previously (Mao et al. 2012).

### Water loss and chlorophyll leaching assays

For water-loss assays, samples were treated as described previously (Qin et al. 2011). Each sample was weighed with a microbalance at 0, 1, 2, 3, 4, 5 and 6 h. The water loss rate was calculated based on the initial weight of the samples.

For chlorophyll leaching measurements, samples were treated according to Mao et al. (2012). The chlorophyll content was quantified with a spectrophotometer (DU-800, Beckman Coulter, USA) at 647 and 664 nm absorption peaks, respectively, according to Lolle et al. (1997).

### Wax and cutin analysis

Cutin monomer analysis was performed according to Li et al. (2010). Leaves that had been used for wax extraction were re-extracted in fresh chloroform/methanol (1:1 v/v)

four times for several hours each. Then the samples were lyophilized. The delipidated samples were then depolymerized using transesterification in 1 mL of 1 N methanolic HCl at 80 °C for 2 h. After the addition of 2 mL of saturated NaCl/$H_2O$ and 10 mg of dotriacontane (Fluka, USA) as an internal standard, the hydrophobic monomers were subsequently extracted three times with 1 mL of hexane. The organic phases were combined, and then the solvent was evaporated. The remaining sample was derivatized and cutin monomers were detected by gas chromatography–mass spectrometry (GC–MS). The cuticular wax was extracted from leaves and analyzed using GC–MS as described previously (Mao et al. 2012).

### Molecular cloning of the *WSL4* gene

All 4-leaf-stage $F_2$ seedlings were immersed in water to identify the extreme water-sticking individuals. A total of 811 leaf wax deficient plants were collected for *WSL4* gene mapping. Genomic DNA was extracted by the CTAB method and the linkage analysis was carried out using both published and newly developed markers (Supplementary Table 1), according to the sequence diversity between Nipponbare and 9311 (*indica* var.) available on Gramene (http://www.gramene.org/).

### Complementation of the *wsl4* mutant

A 7649-bp genomic fragment of *WSL4* containing the full length gene region, the 3902-bp upstream fragment, and 1608-bp downstream fragment was amplified from rice genomic DNA with the primer pairs *WSL4*-2300-C F/R. The PCR product was subcloned into the *Eco*RI/*Sma*I sites of binary vector pCAMBIA2300 using the InFusion Advantage PCR Cloning Kit (Takara, Japan) and sequenced. The complementation vector was introduced into the *wsl4* mutant by *Agrobacterium*-mediated transformation as described previously (Hiei and Komari 2008).

### RNA interference and knock-out of *WSL4*

The RNA interference vector pCUbi1390-$^{\Delta}$FAD2 (ubiqutin promoter and FAD2 intron inserted in pCAMBIA1390) used for RNAi was described previously (Li et al. 2013). A 387-bp pair cDNA fragment was amplified by PCR primer pairs of *WSL4*-1390-RNAi-1 F/R and *WSL4*-1390-RNAi-2 F/R from the cDNA of *WSL4* gene, and then subcloned into the *Sac*I and *Sna*BI sites of the vector pCUbi1390-$^{\Delta}$FAD2. The resulting *WSL4*-RNAi vector construct was introduced into Nipponbare by *Agrobacterium*-mediated transformation.

The high specificity target site for *WSL4*-Crispr was chosen by using the CRISPR-P online website (http://cbi.hzau.edu.cn/cgi-bin/CRISPR) and evaluated the secondary structural of RNA. The forward and reserved primers were mixed in a 1:1 ratio and annealed from 94 to 15 °C at the rate of 0.1 °C/s to form the double strands DNA and integrate into the pCRAC vector. The constructed vector was introduced into Nipponbare by *Agrobacterium*-mediated transformation. Positive T1 lines were subjected to further phenotypic evaluation.

### RNA isolation and quantitative PCR analysis

Total RNA was isolated from WT and transgenic lines using the ZR Plant RNA MiniPrep Kit (Zymo research, USA), following the protocol provide by the manufacturer. 1 μg of RNA was reverse-transcribed into cDNA with the QuantiTech Reverse Transcription Kit (QIAGEN, USA). Quantitative RT-PCR (qRT-PCR) was performed in the 7500 Real-Time PCR System (Applied Biosystems, USA) using the SYBR Green PCR Kit (Takara, Japan) in a reaction volume of 20 μL. The $2^{-\Delta\Delta CT}$ method was used to calculate relative changes in gene expression as described (Rao et al. 2013).

### Subcellular localization and GUS analysis

The coding region of *WSL4* was amplified without the stop codon and cloned into the vector 1305-35S-GFP to generate a WSL4-GFP expression construct under the control of 35S promoter. To investigate the subcellular localization of WSL4 in plant cells, *Agrobacterium* strain EHA105 was transformed with 35S:WSL4-GFP, ER-marker, and P19 vectors, respectively, and cultivated overnight. Then the three *Agrobacteria* were mixed at a ratio of 1:1:1 to a final volume of 1 mL as described (Batoko et al. 2000). After incubating for 4 h in dark, mature *N. benthamiana* leaves were inoculated with the mixture using a syringe. After 2 days inoculation, the protoplasts were isolated by enzyme treatment from the leaf discs. GFP fluorescence was observed at the wavelength of 488 nm under confocal microscope (LSM 700, Carl zeiss, Germany).

For the GUS assay, a 3902-bp upstream fragment of *WSL4* was amplified from rice genomic DNA with primer pair of *WSL4*-1305-GUS F/R. The PCR product was subcloned into the *Eco*RI/*Nco*I site of binary vector pCAMBIA1305 using the InFusion Advantage PCR Cloning Kit. The GUS vector was introduced into the Kitaake by *Agrobacterium*-mediated transformation. Excised tissues from independent transgenic lines were used for GUS activation assay according to the method described previously (Jefferson 1987).

## Results

### Morphological analysis of *wsl4*

To identify critical genes for cuticular wax synthesis in rice, we screened the existing mutant library in our lab, which includes two types mutants generated from EMS mutagenesis and tissue culture-induced mutagenesis, and obtained a tissue culture-induced mutant derived from *Oryza sativa* cv. Nipponbare. The mutant, named as *wax crystal-sparse leaf 4* (*wsl4*), exhibited extreme water adhesiveness (Fig. 1a, b) when seedlings were immersed in water. In addition, *wsl4* was shorter and produced fewer tillers than WT after heading (Fig. 1c, d). $F_1$ hybrids of a cross between *wsl4* and WT exhibited the WT phenotype, and the $F_2$ population was segregated in a 3:1 (WT: *wsl4*) phenotypic ratio, indicating that the *wsl4* phenotype was caused by a single recessive nuclear gene.

### Structural and chemical analysis of cuticular waxes

To investigate the reason for the altered leaf water stickiness phenotype of *wsl4*, the analysis of SEM was performed. There are substantially fewer epicuticular wax crystals on *wsl4* leaf surface, while upright schistose-shaped, pyknotic and regularly wax crystals were arrayed on leaf surface of the wild type (Fig. 2a, b). Similar results were observed on the leaf sheath of *wsl4* (Fig. S1). To further investigate the

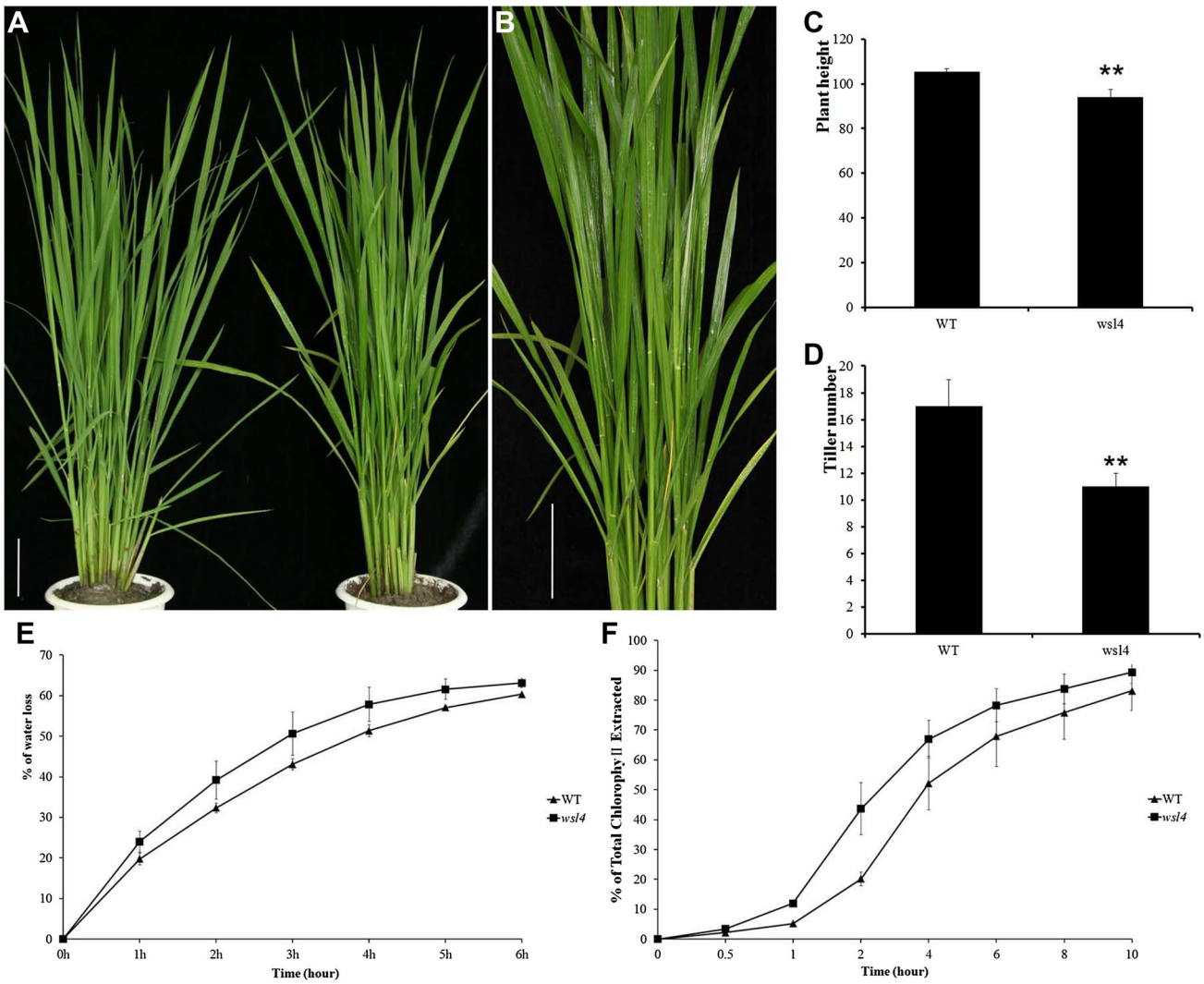


**Fig. 1** Characterization and cuticular permeability of the *wsl4* mutant. **a** Phenotypic comparison of Nipponbare (*left*) and the *wsl4* mutant (*right*); **b** water adhesiveness phenotype of the *wsl4* mutant; **c** plant height (cm) of WT and the *wsl4* mutant; **d** tiller numbers of WT and the *wsl4* mutant; **e** water loss rates of excised leaves of WT and the *wsl4* mutant. Water loss rates were measured at 0, 1, 2, 3, 4, 5 and 6 h. Data are shown as mean ± SE for three replicates; **f** chlorophyll leaching assays of WT and the *wsl4* mutant leaves. Chlorophyll leaching rates of WT and the *wsl4* mutant were measured from 0 to 10 h after immersion in 80% ethanol solution. Data are shown as mean ± SE of three replicates

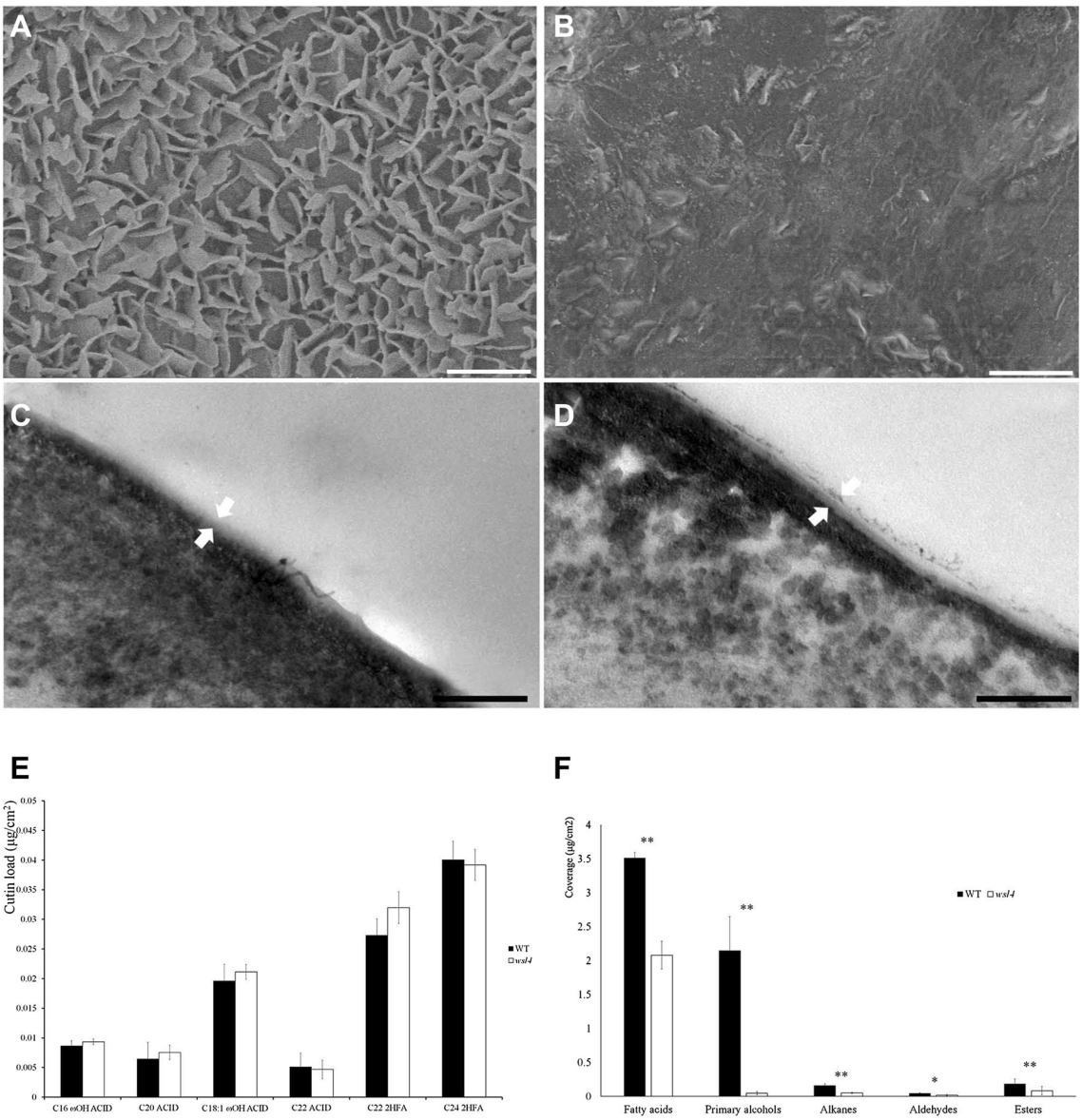


**Fig. 2** Phenotypic analysis of WT and *wsl4*. SEM analysis of epicuticular wax crystal patterns on the leaf surface of WT (**a**) and *wsl4* (**b**). *Bar* 1 μm. TEM analysis of the leaf cuticle membrane of WT (**c**) and *wsl4* (**d**). The leaf cuticle membrane on *wsl4* appears thicker than WT. The cuticle membrane is indicated between the *white arrows*. *Bar* 200 nm. **e** Cutin monomer composition on leaves of WT and *wsl4*. *FA* fatty acid, *ω-OH FA* ω-hydroxyl fatty acid, *2HFA* C16-10,16-dihydroxyl fatty acids, *Error bars* represent ± SE of three biological replicates. **f** Cuticular wax load on the leaf surfaces of WT and the *wsl4* mutant analyzed by GC–MS. *Asterisks* denote significant differences from WT. *Error bars* indicate ±SE ($n = 3$)

ultrastructure of cuticle layers on leaf surface, we performed TEM analysis. The *wsl4* possessed a thicker cuticular layer than the wild type (Fig. 2c, d). Subsequently, GC–MS was employed to analyze the cutin and cuticular wax composition. There were no significant differences in total amount of cutin monomers (Fig. 2e), while the cuticular wax coverage was greatly reduced in leaves of the *wsl4* mutant, compared with the wild type (Fig. 2f).

## Cuticular permeability analysis

We surveyed the cuticle permeability difference between the *wsl4* and the wild type, and the results showed that the excised leaf of *wsl4* lost water significantly faster, and that chlorophyll leached from *wsl4* leaves more quickly than the wild type (Fig. 1e, f). These results suggest that *wsl4* exhibits greater permeability than the WT.

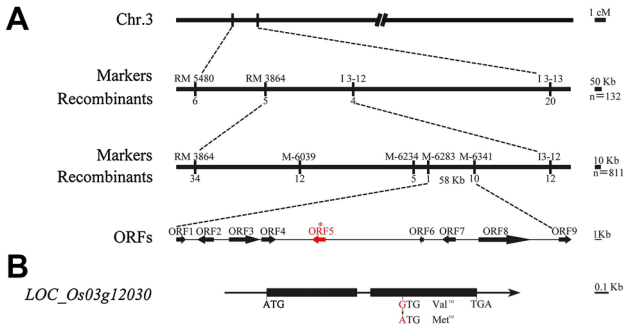


**Fig. 3** Map-based cloning of the *WSL4* locus. **a** Fine mapping of the *wsl4* locus gene on chromosome 3. Markers and the number of recombinants identified are shown. *cM* centimorgan. **b** Schematic gene structure of the *Loc_Os03g12030* gene. The *wsl4* mutant contains a mutation in nucleotides 1281 (G → A) in the second exon of the *Loc_Os03g12030* gene, causing the mutation from $Val^{312}$ to $Met^{312}$

## Map-based cloning of *WSL4*

A total of 811 $F_2$ plants with the mutant phenotype were used for fine mapping of *WSL4*. The mutant site was narrowed to a 58 kb region by the InDel markers M-6283 and M-6341 on chromosome 3 (Fig. 3a). This interval contains nine annotated genes according to the Rice Genome Annotation Project database (http://rice.plantbiology.msu.edu/). A single base mutation (G to A) was found on the fifth open reading frame (ORF) of *LOC_Os03g12030*, causing the 312nd amino acid to change from Val to Met (Fig. 3b). To verify the identity of *WSL4/LOC_Os03g12030* as the candidate gene, a 7742 bp genomic fragment amplified from Nipponbare, including the entire coding region of *LOC_Os03g12030* and its promoter sequences was introduced into *wsl4*. The leaf water-sticking phenotype of transgenic plants was rescued (Fig. 4a) and the wax crystals were also present as WT (Fig. 4b–e). These results indicated that the abnormal phenotypes of *wsl4* are caused by the mutation of *LOC_Os03g12030*, and we therefore designated *LOC_Os03g12030* as *WSL4*.

**Fig. 5** Amino acid sequence alignment and phylogenic analysis of ▶ the WSL4 protein with homologs from other species. **a** The amino acid sequence alignment of WSL4 with homologs from other species. The mutant residue of WSL4 is marked by *asterisk*. **b** The phylogenic analysis of WSL4 with homologs from other species

## Sequence alignment and phylogenetic analysis of WSL4

The WSL4 protein is composed of 494 residues with a predicted molecular mass of 55.79 kDa. The WSL4 protein processes high similarity to the FAE-type KCS family: 90.02% to barley HvCUT1; 78.79% to cotton GhCER6; 78.27% to *Arabidopsis* AtKCS6/CUT1/CER6 and 76.16% to AtKCS5; 77.22% to potato StKCS6/CER6 and 76.81% to tomato LeCER6 (Fig. 5a). The phylogenetic tree based on FAE type KCS members in *Arabidopsis* and rice revealed that WSL4, AtKCS6 and AtKCS5 were located on the same branch (Fig. 5b), suggesting that WSL4 is homologous to KCS6 that catalyzes the first step of elongation reactions of the FAE complex for VLCFAs.

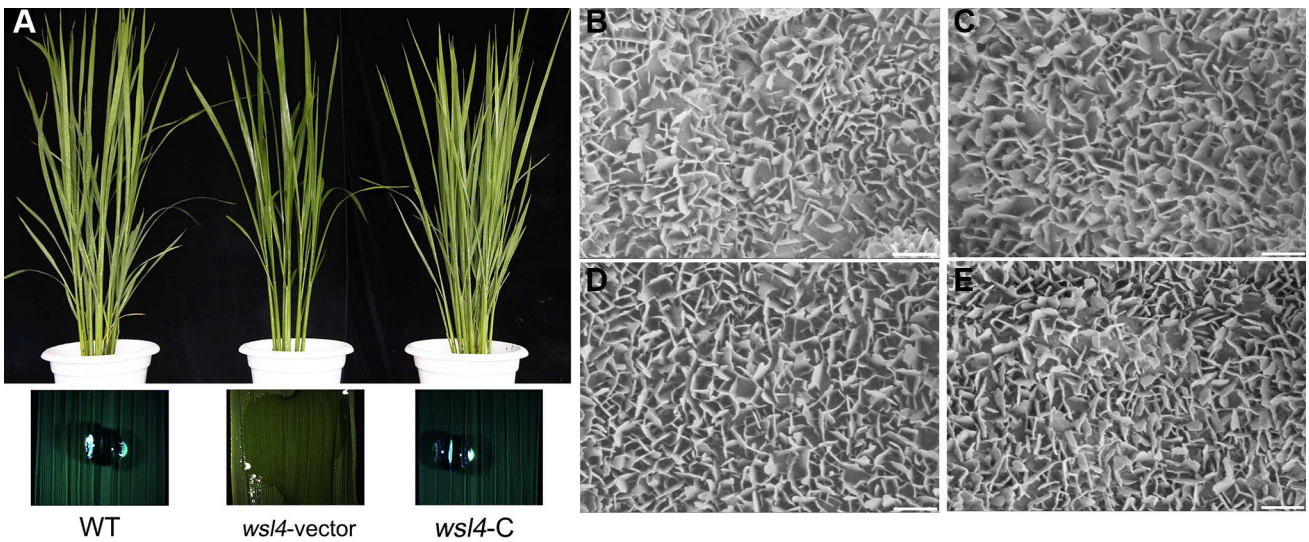


**Fig. 4** Complementation tests of *WSL4*. **a** Phenotypes of transgenic plants in complementation tests. Positive transgenic rice of *wsl4* with a complementary vector containing a 7204 bp genomic fragment of *WSL4* rescues the water adhesive phenotype (*right*) similar to WT (*left*), compared to *wsl4* with an empty vector (*middle*). **b–e** SEM analysis. All three individual complementation tests of transgenic lines in *wsl4* background (**c–e**) show similar wax crystal distributions on leaf surfaces to WT (**b**), *bar* 1 μm

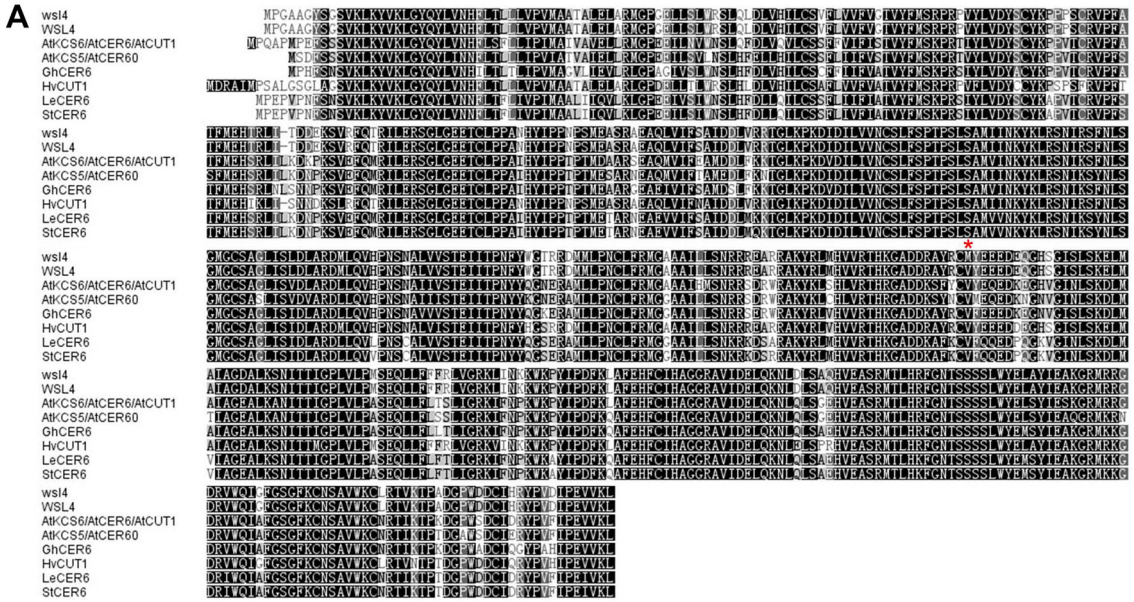
A
wsl4
WSL4
AtKCS6/AtCER6/AtCUT1
AtKCS5/AtCER60
GhCER6
HvCUT1
LeCER6
StCER6

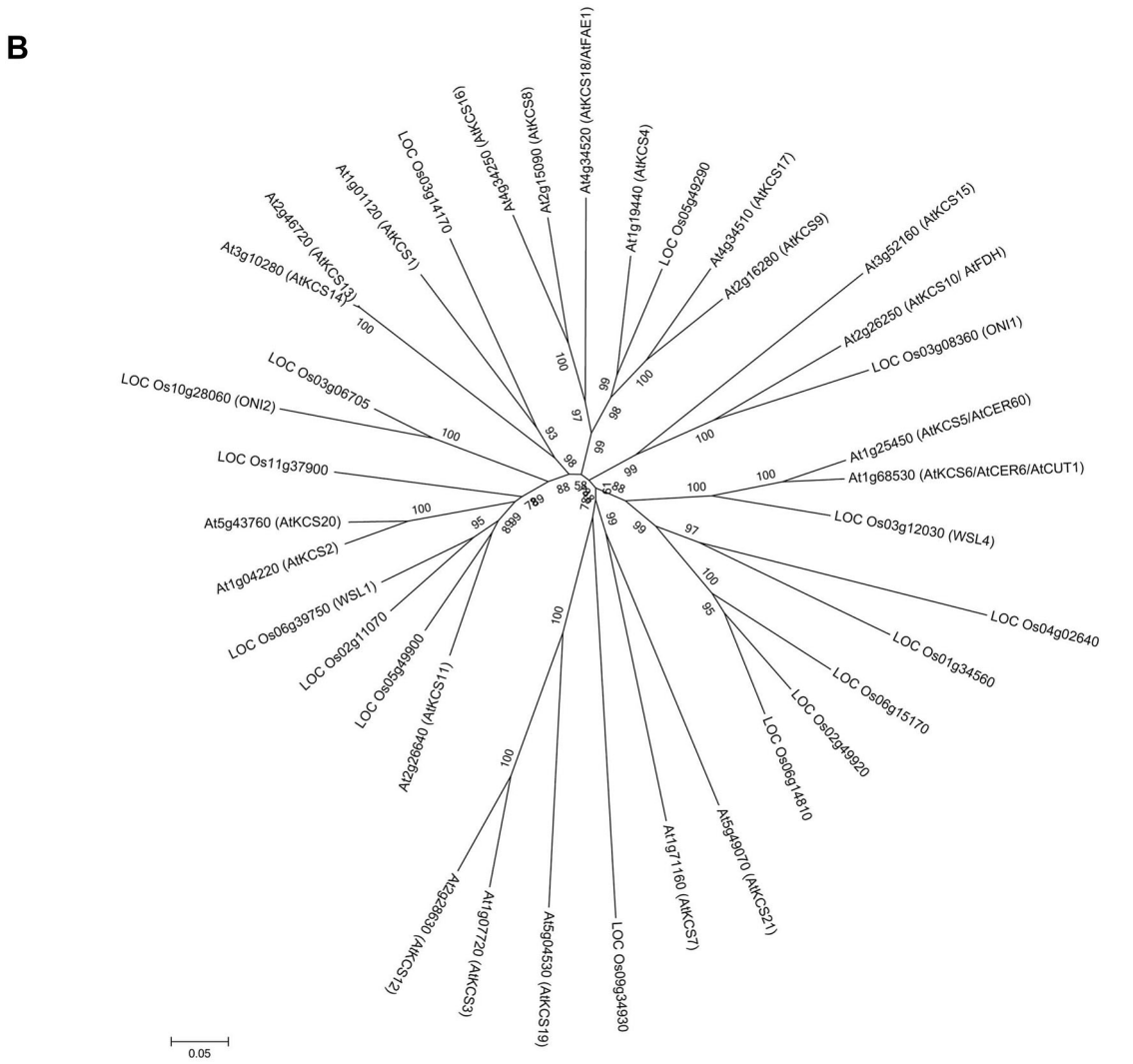
B
At4g34250 (AtKCS16)
At2g15090 (AtKCS8)
At4g34520 (AtKCS18/AtFAE1)
At1g19440 (AtKCS4)
LOC Os05g49290
At4g34510 (AtKCS17)
At2g16280 (AtKCS9)
At3g52160 (AtKCS15)
At2g26250 (AtKCS10/ AtFDH)
LOC Os03g08360 (ONI1)
At1g25450 (AtKCS5/AtCER60)
At1g68530 (AtKCS6/AtCER6/AtCUT1)
LOC Os03g12030 (WSL4)
LOC Os04g02640
LOC Os01g34560
LOC Os06g15170
LOC Os02g49920
LOC Os06g14810
At5g49070 (AtKCS21)
At1g71160 (AtKCS7)
LOC Os09g34930
At5g04530 (AtKCS19)
At1g07720 (AtKCS3)
At2g28630 (AtKCS12)
At2g26640 (AtKCS11)
LOC Os05g49900
LOC Os02g11070
LOC Os06g39750 (WSL1)
At1g04220 (AtKCS2)
At5g43760 (AtKCS20)
LOC Os11g37900
LOC Os10g28060 (ONI2)
LOC Os03g06705
At3g10280 (AtKCS14)
At2g46720 (AtKCS13)
At1g01120 (AtKCS1)
LOC Os03g14170
0.05

### Spatial and temporal expression and subcellular location of WSL4

qRT-PCR analysis showed that *WSL4* was widely expressed in rice leaf, culm, panicle, sheath and young seedling (Fig. 6a). The expression pattern of *WSL4* was further confirmed by GUS staining of $Pro_{WSL4}$*::GUS* transgenic plants. GUS activity was detected in various tissues including root, leaf blade, sheath, stem, lamina joint, glume and flower (Fig. 6b–i). To clarify the subcellular location

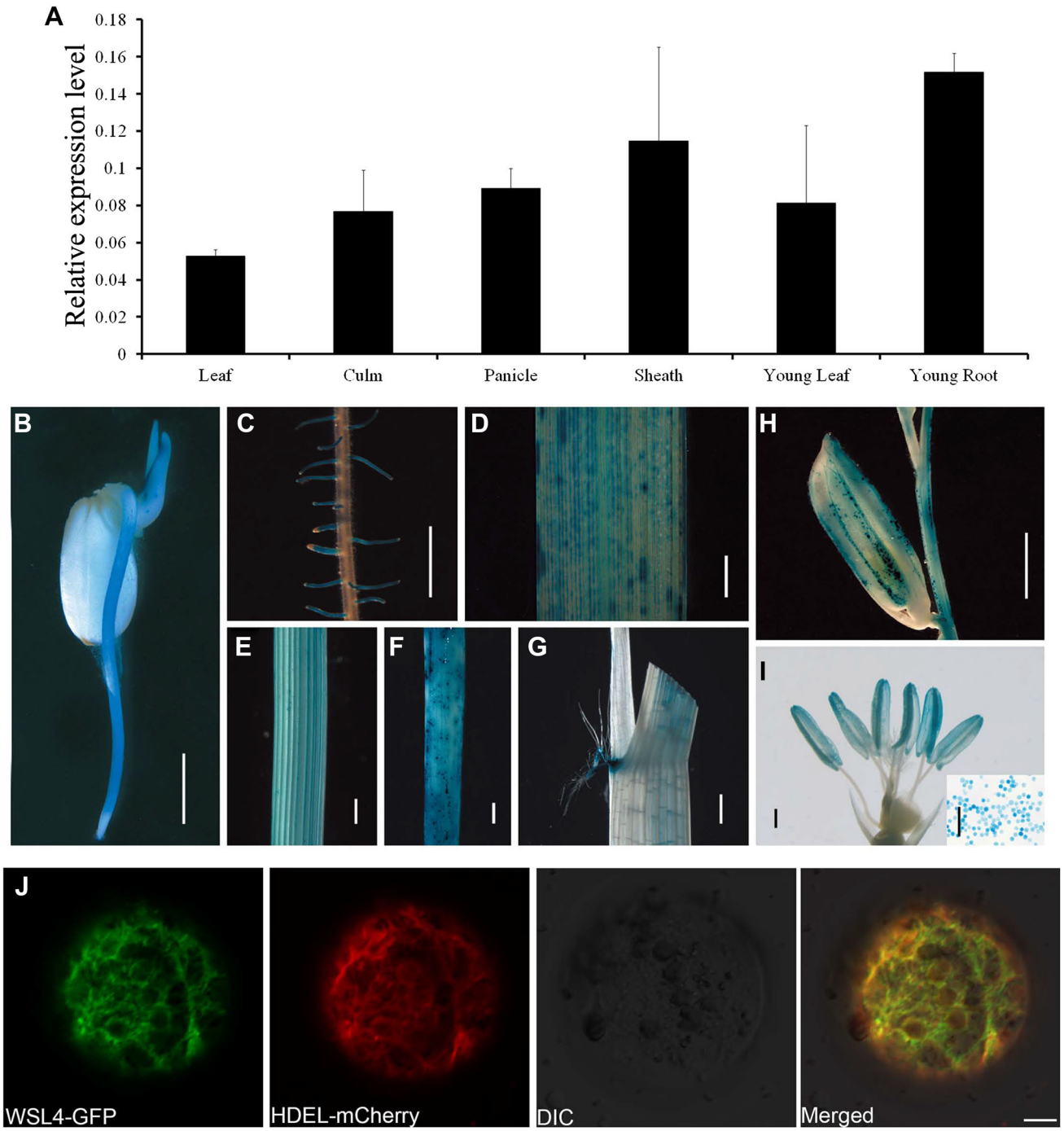


**Fig. 6** Spatial expression pattern of *WSL4* and subcellular location of WSL4. **a** Analysis of *WSL4* expression in different tissues by qRT-PCR. The *UBQ* gene was used as control and *error bars* represent ±SE of three biological replicates. **b–i** Gus expression patterns of $P_{WSL4}$*:GUS* transgenic rice plants. GUS activity was detected in different tissues: plumule (**b**), root (**c**), leaf blade (**d**), sheath (**e**), stem (**f**), lamina joint (**g**), glume (**h**), and flower (**i**). **b–h** *Bar* 1 mm, **i** *bar* 1 μm. **j** Co-expression of WSL4-GFP fusion protein and the HDEL-mCherry fusion protein in *N. benthamiana* protoplasts was imaged by confocal microscopy with a Zeiss LSM700 fitted with *green* (WSL4-GFP) and *red* filters (HDEL-mCherry) (color figure online)

of WSL4, we transiently expressed the WSL4-GFP fusion protein in tobacco leaves. The green fluorescent signals from WSL4-GFP co-localized with the ER marker mCherry-HDEL, indicating WSL4 is localized in the ER (Fig. 6j).

### RNA interference and knocked-out of *WSL4*

To further confirm the function of WSL4 involved in wax biosynthesis in rice, the *WSL4*-RNAi transgenic plants and *WSL4*-targeted knocked-out mutant lines in Nipponbare were constructed. The leaf cuticular wax density of these plants was examined with SEM. The RNAi transgenic lines showed obvious leaf water-sticking phenotype (Fig. 7a). The expression of *WSL4* in RNAi transgenic lines was greatly decreased (Fig. 7b). Besides, the SEM analyses of RNAi transgenic lines revealed substantial reduction in wax crystal density (Fig. 7d–f). Furthermore, all *WSL4* knocked-out mutants exhibited wax load decrease on the leaf surface comparing to the WT (Fig. 7g–i). All these data suggest that *WSL4* is required for cuticular wax accumulation in rice.

## Discussion

In this study, we showed that *WSL4* encodes a KCS6 which is involved in the VLCFAs elongation reactions. Comparing to the WT, *wsl4* displays reduced surface wax loads. Map-based cloning and nucleotide sequencing results revealed that the phenotype of *wsl4* is caused by a single nucleotide substitution in the second exons of *LOC_Os03g12030*, causing a conservative amino acid alternation of the whole peptide. Genetic complementation confirmed that the mutation in *WSL4* was responsible for the mutant phenotype. Bioinformatics analysis indicated that WSL4 belongs to the KCS family and is highly homologous to AtKCS6/CUT1/CER6 (Millar et al. 1999; Fiebig et al. 2000), HvKCS6/CUT1.3 (Weidenbach et al. 2014), StKCS6 (Serra et al. 2009), LeCER6 (Leide et al. 2007) and GhCER6 (Qin et al. 2007), most of which were previously validated as one of the FAE complex involved in the first step of VLCFA elongation reactions.

In rice, three other KCS genes, *WSL1*, *ONI1* and *ONI2,* have been cloned. The T-DNA insertion mutant *wsl1* exhibits a pleiotropic phenotype including sparse wax crystals. *WSL1* encodes a protein of KCS family and is ubiquitously expressed in rice, the VLCFA precursors of C20–C24 of total wax load are reduced on both leaf blades and sheathes in *wsl1* (Yu et al. 2008). *ONI1* encodes a fatty acid elongase similar to *AtFDH* which functions in the synthesis of VLCFAs. *oni1* produces very small shoots, lethal seedlings, and an aberrant outermost epidermal cell layer due to reducing the amount of VLCFAs and alcohols components in wax (Ito et al. 2011). *ONI2* encodes another rice KCS family gene, the *oni2* mutant has a reduced amount of VLCFAs and is characterized by growth cessation after germination, fused leaves, and small shoots (Tsuda et al. 2013). Both studies on *ONI1* and *ONI2* suggest that VLCFAs play an important role for normal development in rice. In our study, the *wsl4* mutants also exhibit significant reduced wax load comparing to the WT.

In *Arabidopsis*, the *KCS6*/*CUTI*/*CER6* gene encodes a VLCFA condensing enzyme which localizes in the epidermis cells and determines long-chain lipid content on the pollen and stems surface (Millar et al. 1999; Fiebig et al. 2000), especially for the production of C28 VLCFAs (Millar et al. 1999; Haslam et al. 2012). One *WSL4* homolog in barley is *HvCUT1.3* (*HvKCS6*). Its mutant *emr1* has significantly fewer aliphatic wax constituents longer than C24 (Weidenbach, et al. 2014). In cotton, heterologous expression of the *Arabidopsis* protein homolog encoding gene *GhCER6* in yeasts could rescue growth defect phenotypes of both *elo3* deletion mutant and *elo2*-Δ*elo3*Δ double mutant, accompanied by detectable increase in the amount of VLCFAs products ranged from C20 to C26, suggesting GhCER6 is a functional β-ketoacyl-CoA synthase (Qin et al. 2007). *lecer6* of tomato exhibits up to three- to eightfold water loss comparing to the wild type, due to the C28 VLCFAs decrease in fruit cuticular waxes constitutions (Leide et al. 2007). In potato, RNAi lines of *StKCS6*, all VLCFAs compounds with chain length shorter than C26 are accumulated. On the contrary, the components with chain length longer than C28 are significantly reduced. These indicated that *StKCS6* is essential for the formation of lipid monomers with chain lengths longer than C28 in both suberin and wax biosynthesis (Serra et al. 2009). Because different KCS genes have different substrate specificities, loss function of one KCS gene may interrupt the fatty acid elongation and then effect wax load. In the present study, we found that *WSL4* encodes a rice KCS6 homologous protein, and the *wsl4* mutant displays significant reduced wax loads on leaf surface, consistent with the function of other KCSs in previous studies.

Both the *WSL4-RNAi* transgenic lines and *WSL4* knocked-out mutants could mimic the phenotypes of *wsl4* in cuticular wax decrease, confirming that *WSL4* is indispensable in rice cuticular wax biosynthesis. The qRT-PCR and GUS assay indicated that *WSL4* is expressed ubiquitously, similar to expression pattern of other two KCSs, viz. *KCS1* and *KCS9* in *Arabidopsis* (Todd et al. 1999; Kim et al. 2013). Transient expression of the WSL4-GFP fusion protein in tobacco revealed a reticulate network subcellular localization, corresponding to the FAE subunits localization in the ER network (Joubès et al. 2008).

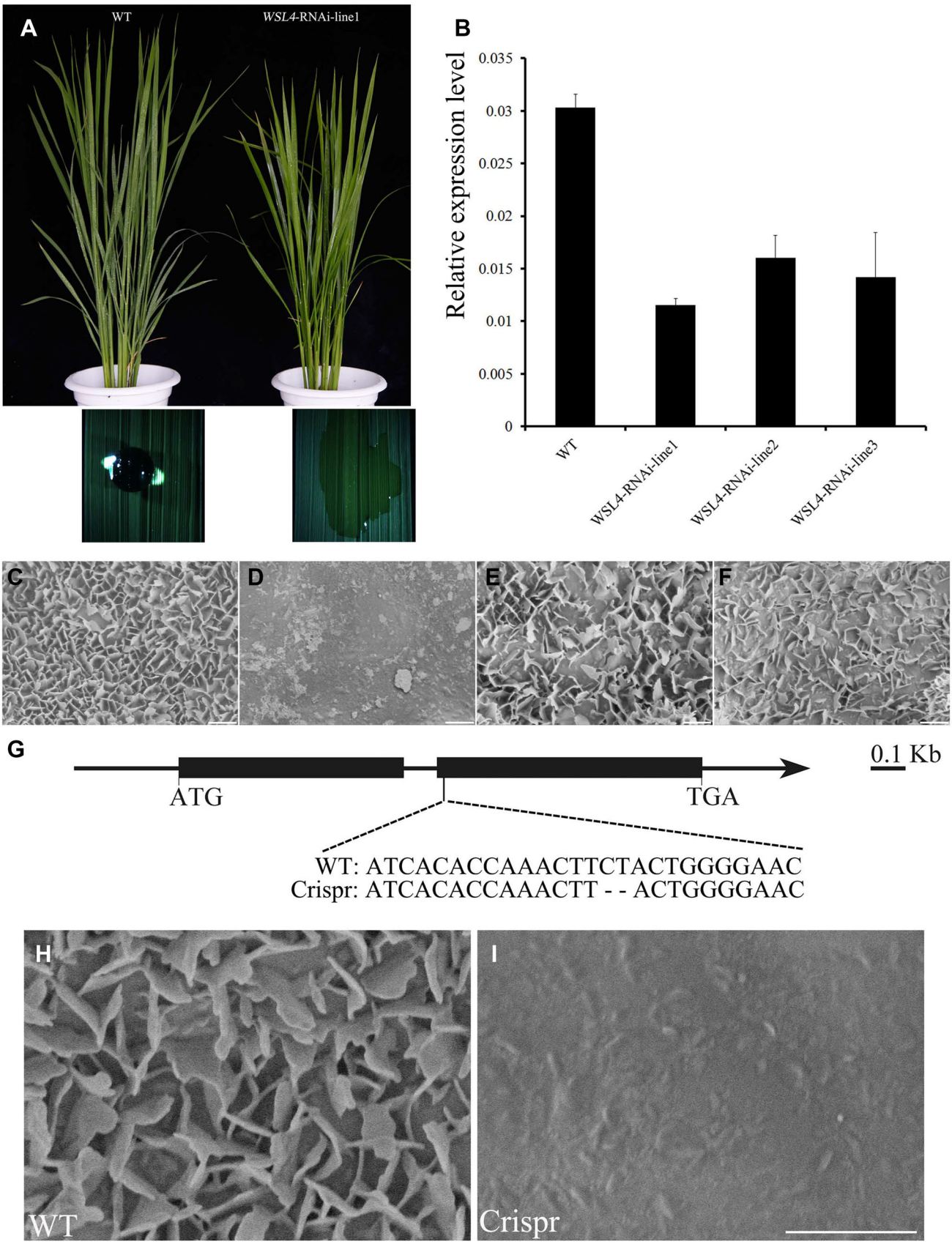
A
WT
WSL4-RNAi-line1
B
Relative expression level
0.035
0.03
0.025
0.02
0.015
0.01
0.005
0
WT
WSL4-RNAi-line1
WSL4-RNAi-line2
WSL4-RNAi-line3
C
D
E
F
G
0.1 Kb
ATG
TGA
WT: ATCACACCAAACTTCTACTGGGGAAC
Crispr: ATCACACCAAACTT - - ACTGGGGAAC
H
WT
I
Crispr

◀**Fig. 7** RNAi and Knocked-out of *WSL4* in rice. **a** Phenotypic comparison of Nipponbare (*left*) and *WSL4*-RNAi transgenic plants (*right*). **b** Expression analysis of the *WSL4* gene in different RNAi transgenic lines and WT by qRT-PCR. The *UBQ* gene was used as the control; *error bars* represent ± SE of three biological replicates. **c**–**f** SEM analysis of *WSL4*-RNAi plants and WT. All three individual *WSL4*-RNAi transgenic lines (**d**–**f**) in Nipponbare background show significantly decreased wax crystals on the leaf surface compared to WT (**c**). **g** Sequence analysis of *WSL4*-knocked-out transgenic plants. **h**, **i** SEM analysis of the WT and *WSL4*-knocked-out transgenic plants, *bar* 1 μm

In conclusion, this study demonstrated that *WSL4* encoding a KCS6 protein is involved in rice leaf cuticular wax formation. The biochemical function of WSL4 in the synthesis of rice suberins, sphingolipids and phospholipids deserves further study.

**Author contribution statement** LG, SSZ, ZCZ, and JMW designed the research. LG, SSZ, ZCZ, LLL, XLW and ZZ performed the research. XZ, JW, JLW and XPG managed the rice transformation. LG, SSZ, ZCZ, LLL and JMW wrote the paper.

**Acknowledgements** This work was supported by the National Key R&D Program of China (2016YFD0100600, 2016YFD0200700), and the National Special Project of China (2014ZX08001-006).

**Compliance with ethical standards**

**Conflict of interest** The authors declare that they have no conflict of interests.

## References

Aharoni A, Dixit S, Jetter R, Thoenes E, van Arkel G, Pereira A (2004) The SHINE clade of AP2 domain transcription factors activates wax biosynthesis, alters cuticle properties, and confers drought tolerance when overexpressed in *Arabidopsis*. Plant Cell 16:2463–2480

Batoko H, Zheng HQ, Hawes C, Moore I (2000) A rab1 GTPase is required for transport between the endoplasmic reticulum and golgi apparatus and for normal golgi movement in plants. Plant Cell 12:2201–2218

Buschhaus C, Jetter R (2012) Composition and physiological function of the wax layers coating *Arabidopsis* leaves: β-amyrin negatively affects the intracuticular water barrier. Plant Physiol 160:1120–1129

Espana L, Heredia-Guerrero JA, Reina-Pinto JJ, Fernandez-Munoz R, Heredia A, Dominguez E (2014) Transient silencing of CHALCONE SYNTHASE during fruit ripening modifies tomato epidermal cells and cuticle properties. Plant Physiol 166:1371–1386

Fiebig A, Mayfield JA, Miley NL, Chau S, Fischer RL, Preuss D (2000) Alterations in CER6, a gene identical to CUT1, differentially affect long-chain lipid content on the surface of pollen and stems. Plant Cell 12:2001–2008

Haslam TM, Kunst L (2013) Extending the story of very-long-chain fatty acid elongation. Plant Sci 210:93–107

Haslam TM, Manas-Fernandez A, Zhao L, Kunst L (2012) *Arabidopsis* ECERIFERUM2 is a component of the fatty acid elongation machinery required for fatty acid extension to exceptional lengths. Plant Physiol 160:1164–1174

Hiei Y, Komari T (2008) Agrobacterium-mediated transformation of rice using immature embryos or calli induced from mature seed. Nat Protoc 3:824–834

Hooker TS, Millar AA, Kunst L (2002) Significance of the expression of the CER6 condensing enzyme for cuticular wax production in *Arabidopsis*. Plant Physiol 129:1568–1580

Ito Y, Kimura F, Hirakata K, Tsuda K, Takasugi T, Eiguchi M, Nakagawa K, Kurata N (2011) Fatty acid elongase is required for shoot development in rice. Plant J 66:680–688

James DW Jr, Lim E, Keller J, Plooy L, Ralston E, Dooner HK (1995) Directed tagging of the *Arabidopsis FATTY ACID ELONGATIONl* (*FAEl*) gene with the maize transposon activator. Plant Cell 7:309–319

Jefferson RA (1987) Assaying chimeric genes in plants: the GUS gene fusion system. Plant Mol Biol Rep 5:387–405

Jetter R, Schaffer S (2001) Chemical composition of the *Prunus laurocerasus* leaf surface. Dynamic changes of the epicuticular wax film during leaf development. Plant Physiol 126:1725–1737

Joubès J, Raffaele S, Bourdenx B, Garcia C, Laroche-Traineau J, Moreau P, Domergue F, Lessire R (2008) The VLCFA elongase gene family in *Arabidopsis thaliana*: phylogenetic analysis, 3D modelling and expression profiling. Plant Mol Biol 67:547–566

Kannangara R, Branigan C, Liu Y, Penfield T, Rao V, Mouille G, Hofte H, Pauly M, Riechmann JL, Broun P (2007) The transcription factor WIN1/SHN1 regulates Cutin biosynthesis in *Arabidopsis thaliana*. Plant Cell 19:1278–1294

Kim J, Jung JH, Lee SB, Go YS, Kim HJ, Cahoon R, Markham JE, Cahoon EB, Suh MC (2013) *Arabidopsis* 3-ketoacyl-coenzyme a synthase9 is involved in the synthesis of tetracosanoic acids as precursors of cuticular waxes, suberins, sphingolipids, and phospholipids. Plant Physiol 162:567–580

Kunst L, Samuels L (2009) Plant cuticles shine: advances in wax biosynthesis and export. Curr Opin Plant Biol 12:721–727

Lee SB, Suh MC (2013) Recent advances in cuticular wax biosynthesis and its regulation in *Arabidopsis*. Mol Plant 6:246–249

Lee S, Jung S, Go Y, Kim H, Kim J, Cho H, Park OK, Suh M (2009) Two *Arabidopsis* 3-ketoacyl CoA synthase genes, KCS20 and KCS2/DAISY, are functionally redundant in cuticular wax and root suberin biosynthesis, but differentially controlled by osmotic stress. Plant J 60:462–475

Leide J, Hildebrandt U, Reussing K, Riederer M, Vogg G (2007) The developmental pattern of tomato fruit wax accumulation and its impact on cuticular transpiration barrier properties: effects of a deficiency in a beta-ketoacyl-coenzyme A synthase (LeCER6). Plant Physiol 144:1667–1679

Li H, Pinot F, Sauveplane V, Werck-Reichhart D, Diehl P, Schreiber L, Franke R, Zhang P, Chen L, Gao Y, Liang W, Zhang D (2010) Cytochrome P450 family member CYP704B2 catalyzes the ω-hydroxylation of fatty acids and is required for anther cutin biosynthesis and pollen exine formation in rice. Plant Cell 22:173–190

Li H, Jiang L, Youn JH, Sun W, Cheng Z, Jin T, Ma X, Guo X, Wang J, Zhang X, Wu F, Wu C, Kim SK, Wan J (2013) A comprehensive genetic study reveals a crucial role of CYP90D2/D2 in regulating plant architecture in rice (*Oryza sativa*). New Phytol 200:1076–1088

Li-Beisson Y, Shorrosh B, Beisson F, Andersson MX, Arondel V, Bates PD, Baud S, Bird D, Debono A, Durrett TP, Franke RB, Graham IA, Katayama K, Kelly AA, Larson T, Markham JE, Miquel M, Molina I, Nishida I, Rowland O, Samuels L, Schmid

KM, Wada H, Welti R, Xu C, Zallot R, Ohlrogge J (2013) Acyl-lipid metabolism. Arabidopsis Book 11:e161

Lolle SJ, Berlyn GP, Engstrom EM, Krolikowski KA, Reiter WD, Pruitt RE (1997) Developmental regulation of cell interactions in the *Arabidopsis* fiddlehead-1 mutant: a role for the epidermal cell wall and cuticle. Dev Biol 189:311–321

Mao B, Cheng Z, Lei C, Xu F, Gao S, Ren Y, Wang J, Zhang X, Wang J, Wu F, Guo X, Liu X, Wu C, Wang H, Wan J (2012) *Wax crystal-sparse leaf*2, a rice homologue of WAX2/GL1, is involved in synthesis of leaf cuticular wax. Planta 235:39–52

Millar AA, Clemens S, Zachgo S, Giblin EM, Taylor DC, Kunst L (1999) CUT1, an *Arabidopsis* gene required for cuticular wax biosynthesis and pollen fertility, encodes a very-long-chain fatty acid condensing enzyme. Plant Cell 11:825–838

Paul S, Gable K, Beaudoin F, Cahoon E, Jaworski J, Napier JA, Dunn TM (2006) Members of the *Arabidopsis* FAE1-like 3-ketoacyl-CoA synthase gene family substitute for the Elop proteins of *Saccharomyces cerevisiae*. J Biol Chem 281:9018–9029

Qin YM, Pujol FM, Hu CY, Feng JX, Kastaniotis AJ, Hiltunen JK, Zhu YX (2007) Genetic and biochemical studies in yeast reveal that the cotton fibre-specific *GhCER6* gene functions in fatty acid elongation. J Exp Bot 58:473–481

Qin B, Tang D, Huang J, Li M, Wu X, Lu L, Wang K, Yu H, Chen J, Gu M, Cheng Z (2011) Rice OsGL1-1 is involved in leaf cuticular wax and cuticle membrane. Mol Plant 4(6):985–995

Rao X, Huang X, Zhou Z, Lin X (2013) An improvement of the 2^(−delta delta CT) method for quantitative real-time polymerase chain reaction data analysis. Biostat Bioinform Biomath 3:71–85

Samuels L, Kunst L, Jetter R (2008) Sealing plant surfaces: cuticular wax formation by epidermal cells. Annu Rev Plant Biol 59:683–707

Serra O, Soler M, Hohn C, Franke R, Schreiber L, Prat S, Molinas M, Figueras AM (2009) Silencing of *StKCS6* in potato periderm leads to reduced chain lengths of suberin and wax compounds and increased peridermal transpiration. J Exp Bot 2:697–707

Shepherd T, Wynne Griffiths D (2006) The effects of stress on plant cuticular waxes. New Phytol 171:469–499

Sieber P, Schorderet M, Ryser U, Buchala A, Kolattukudy P, Metraux JP, Nawrath C (2000) Transgenic *Arabidopsis* plants expressing a fungal cutinase show alterations in the structure and properties of the cuticle and postgenital organ fusions. Plant Cell 12:721–738

Sturaro M, Hartings H, Schmelzer E, Velasco R, Salamini F, Motto M (2005) Cloning and characterization of *GLOSSY1*, a maize gene involved in cuticle membrane and wax production. Plant Physiol 138:478–489

Todd J, Post-Beittenmiller D, Jaworski JG (1999) *KCS1* encodes a fatty acid elongase 3-ketoacyl-CoA synthase affecting wax biosynthesis in *Arabidopsis thaliana*. Plant J 2:119–130

Tsuda K, Akiba T, Kimura F, Ishibashi M, Moriya C, Nakagawa K, Kurata N, Ito Y (2013) ONION2 fatty acid elongase is required for shoot development in rice. Plant Cell Physiol 54:209–217

Weidenbach D, Jansen M, Franke RB, Hensel G, Weissgerber W, Ulferts S, Jansen I, Schreiber L, Korzun V, Pontzen R, Kumlehn J, Pillen K, Schaffrath U (2014) Evolutionary conserved function of barley and *Arabidopsis* 3-KETOACYL-CoA SYNTHASES in providing wax signals for germination of powdery mildew fungi. Plant Physiol 166:1621–1633

Yeats TH, Rose JKC (2013) The formation and function of plant cuticles. Plant Physiol 163:5–20

Yu D, Ranathunge K, Huang H, Pei Z, Franke R, Schreiber L, He C (2008) *Wax Crystal-Sparse Leaf1* encodes a β-ketoacyl CoA synthase involved in biosynthesis of cuticular waxes on rice leaf. Planta 228(4):675–685